OPTIMAL CONSTRAINED VISCOELASTIC TAPE LENGTHS FOR MAXIMIZING DAMPING IN LAMINATED COMPOSITES

P. RAJU MANTENA, RONALD F. GIBSON and SHWILONG J. HWANG
Department of Mechanical Engineering,
University of Idaho,
Moscow, Idaho 83843.

ABSTRACT

In this paper, the results of experimental investigations conducted on glass/epoxy and graphite/epoxy composite laminated beams with constrained layer surface damping treatments, are reported. The Fast Fourier Transform based impulse technique is used for identifying an optimal length of damping tape to be applied for maximizing the structural loss factor. This requirement stems from a need (as in helicopter rotor blade applications) for a trade-off between the added weight of the viscoelastic layer and the resultant changes in the dynamic characteristics of the structure.

The experimental data is compared with analytical results obtained by a modal strain energy/three dimensional finite element method. This study has shown that, for a given composite structure and boundary conditions there exists an optimum length of the constraining layer which produces maximum shear deformation of the intermediate viscoelastic damping layer, thus providing effective vibration control in severe dynamic environments.

INTRODUCTION

Surface damping treatments have been in vogue for quite some time for solving a variety of resonant noise and vibration problems - especially those associated with sheet metal structure vibration. Such treatments, which capitalize on the inherent damping of a highly dissipative material, can easily be applied as a single layer (as with auto undercoatings) to one or both sides of existing structures and provide high damping capability over a wide temperature and frequency range. In case of the free-layer (also referred to as extensional or unconstrained) damping treatment, when the base plate bends the amount of energy absorbed per oscillation depends on the mean longitudinal strain induced in the coating. Degree of damping is therefore limited by thickness and weight restrictions.

On the other hand, for a given weight, the shear type of damping treatment, which can be obtained by the application of commercially available damping tapes to the base structure, is found to be more efficient than the unconstrained-layer damping treatment. This efficiency is balanced, however, by greater complications in analysis and application. The treatment is similar to the unconstrained-layer type except that the viscoelastic material is constrained by a metal layer. Therefore, whenever the structure is subjected to cyclic bending, the thin and extensionally stiff metal foil placed on top of a thin layer of dissipative material (an adhesive, for example), constrains the viscoelastic layer, thus forcing it to deform in shear. Since shear deformation is considered to be one of the major mechanisms by which energy is dissipated in polymeric adhesives, the large shear strains so produced provide considerable damping. This is the basic principle that is exploited in constrained layer damping treatments.

For facilitating the desired performance, parameters other than temperature and frequency, namely geometry, stiffness, mass and resonance mode shape of the structure to which the control system is applied will also equally effect the performance. The methods of analysis for such free-layer and constrained layer damping systems were developed by Ross-Kerwin-Ungar (referred to as the RKU analysis) in the sixties[1] and have been most widely used for predicting the structural response under both extensional and shear deformations. Application of this RKU method with improvements and/or modifications thereof for noise reduction in helicopter cabins, in diesel engines, for vibration control in a jet engine inlet guide-vanes and in aircraft weapons dispensers are reported by Jones[2,3], Rogers and Nashif[4], Nashif, Jones and Parin[5], and Nashif and Nicholas[6], respectively. Ely reports of advanced designs[7,8] for an A-7 center section and the F-111 outboard spoiler using constrained layer damping treatment which extended their service life by a factor of at least fifty. About one-half of that improvement was attributed to constrained layers of AF-32 adhesive, the remainder of the improvement was due to changes in materials, shapes, forming and fastening.

Almost all the reported applications were designed, however, to improve the dynamic response of metallic structural elements. To the authors' knowledge, there have been a very limited number of previous applications[9] of constrained layer damping treatments for vibration control of composite structural elements. In the recent past, an exhaustive study of the optimization of the internal material damping of various types of advanced composites has been undertaken, both at the University of Idaho and at other research institutions. These analytical and experimental investigations included aligned short fiber composites[10,11]; aligned short

fiber off-axis composites[12-14]; randomly oriented short fiber composites[15]; and two and three dimensional modeling of laminated composites[16-20]. Parameters such as loading angle, fiber aspect ratio, fiber tip spacing, ply thickness, and damping ratio between the fiber and matrix materials were adjusted to improve the performance of composite materials in a dynamic environment.

OBJECTIVE AND SCOPE OF RESEARCH

Designs generated by parametric studies of the type described above are, however, at best locally optimal with improvements of internal material damping being restricted by the properties of the fiber and matrix materials, along with an inherent trade-off between damping and stiffness. Many of the composite structures used in military and space applications, however, are subjected to severe dynamic loading environments where such a trade-off may not be desirable. With enhancement of internal material damping having already been exploited to its peak level by the methods described above, further vibration control by the use of surface damping treatments to reduce resonant displacements and noise level provides the scope for exploratory studies of the type reported in this paper.

As such, the objective of this research was to demonstrate the potential for improvement and optimization of damping in laminated anisotropic composite structures with constrained viscoelastic layer damping tapes. The influence of damping tape distribution and boundary conditions on damping of different modes, in unidirectional and off axis glass/epoxy and graphite/epoxy composite beams were investigated. Experimental data generated by a Fast Fourier Transform based impulse technique was compared with analytical predictions obtained by a modal strain energy / three dimensional finite element method.

EXPERIMENTAL PROCEDURES

A 12 inches (304.8 mm) x 12 inches (304.8 mm), 16 ply unidirectional aligned continuous E-glass/epoxy (3M Scotchply 1003) composite plate with a thickness of 0.13 inches (3.3 mm) was fabricated as per manufacturer's specifications, using an autoclave-style process[21]. Cantilever beam specimens 5 inches long (127 mm) x 1 inch wide (25.4 mm) were machined from this plate. Similarly, unidirectional and 20^0 off-axis graphite/epoxy specimens having dimensions of 8 inches (203.2 mm) long x 0.75 inches (19.05 mm) wide x 0.057 inches (1.45 mm) thick were machined from a laminated plate fabricated with 12 plies of Fiberite Hy-E1034C (T300 graphite fibers / 934 epoxy resin) prepreg tape. Base line loss factor data was obtained for these bare specimens (comprising the base structure, i.e without damping tape) by testing them as cantilever beams for different span lengths (to get the frequency dependency) using the impulse-frequency response vibration technique.

In the impulse-frequency response technique, the specimen is excited by using an impulse hammer with a piezo-electric force transducer in its tip. The specimen response is measured by a non-contacting eddy current proximity transducer, located away from the nodal points. By curve fitting the resonant peak of the Fourier Transformed frequency response function displayed on the screen of the spectrum analyzer, the loss factor (a measure of damping) of the composite specimens is obtained with the half-power bandwidth relationship :

$$\eta = \frac{\Delta f}{f_n} \qquad (1)$$

where Δf = half-power bandwidth of resonant peak frequency response curve at resonant frequency f_n.

For further details of the impulse-frequency response technique the reader is referred to Reference 22.

Damping tape (3M type SJ-2052X) having a 0.005 inches (0.127 mm) thick ISD 112 acrylic polymer viscoelastic adhesive and a 0.01 inches (0.254 mm) thick dead soft aluminum backing as the constraining layer was then applied on one side of the glass/epoxy and graphite/epoxy specimens comprising the base structure for different ratios of tape length to cantilever beam length. Loss factor data was again obtained for different boundary conditions such as tape fixed at root (i.e at clamped end), tape free at root and for tape applied about 0.5 inches (12.7 mm) from the clamped end, as shown in Figure 1. Both first and second mode loss factor data was obtained, with three specimens tested in each category.

MODAL STRAIN ENERGY / FINITE ELEMENT METHOD

The resulting experimental data was compared with the analytical predictions obtained by a modal strain energy / three dimensional finite element method. The strain energy method has been proven to be an accurate and flexible technique for determining damping of structures. The concept of damping in terms of strain energy quantities was apparently first introduced by Ungar and Kerwin[23] and was later implemented in finite element analysis[18,24,25]. In the current research, this method was used in a three-dimensional finite element formulation for determining the loss factor of the composite beam specimens with variations of cross-section (due to application of damping tape for different ratios of tape to beam length) and boundary conditions. The finite element code used in this work is the SAP IV finite element program[26] which was modified for the calculation of the loss factor by the strain energy method[19,20]. For more details of this three dimensional modal strain energy / finite element technique, the reader is referred to References 19,20.

By this approach, an eigenvalue/eigenvector problem for free undamped vibration is performed with the finite element method. The structural loss factor for each mode of vibration is calculated by using the mode shape and the material loss factor for each material. That is, strain energies are calculated based on the resulting eigenvector (mode shape) without concerning the real amplitude of the mode shape. The loss factor of the overall structure (with the applied damping treatment) may therefore be formulated as the weighted average of the loss factors of the constituents (i.e. base structure, damping layer and constraining layer) along with their respective strain energies as weighting constants. Thus the structural loss factor at a macro-mechanical level may be expressed as :

$$\eta_s = \frac{\eta_a W_a + \eta_b W_b + \eta_c W_c}{W_a + W_b + W_c} \qquad (2)$$

where η is the loss factor, W is the strain energy and subscripts s,a,b, and c refer to the total structure, adhesive layer, base (composite) structure and constraining layers, respectively. Due to the anisotropic nature of the composite base structure, further decomposition of the strain energy terms into terms associated with different stress components is also required[19,20].

Based on some initial strain energy convergence studies, optimum aspect ratios (length/thickness) of the three-dimensional eight-node thick shell elements used for modeling the different layers that constitute the composite structure were selected. Figure 2 shows a typical gridwork for a composite specimen with a damping tape-to-beam length ratio of 0.6 and with a free boundary condition at the clamped end. Solution times for such a configuration and related models ranged from 250 to 500 seconds (CPU) on an IBM 4341 main frame system. Constituent material properties used in the analytical models are shown in Table 1. Because of the frequency and temperature sensitivity of both the shear modulus and loss factor of the ISD 112 viscoelastic adhesive in the damping tape, appropriate data based on nomographs supplied by the manufacturer[27] and Reference 28 was used to account for the differences in mode 1 and mode 2 frequencies. Also the Poisson's ratio for the nearly incompressible viscoelastic adhesive was taken as 0.49 (instead of 0.5), to avoid numerical difficulties[29].

RESULTS AND DISCUSSION

As can be observed in Figure 3, for the first mode of vibration, an optimized length of the viscoelastic material at which the system damping (glass/epoxy base structure with tape) is maximum is clearly evident for both the boundary conditions of tape fixed and tape free at root (i.e at the clamped end with N/L = 0). Of particular interest is that for an optimum tape-to-beam length ratio of 0.5, the system damping is significantly higher for the case where the tape is fixed at the root (by about 15 times) than for the case where the tape is free at root. The existence of an optimized length of viscoelastic material for which the structural damping is maximum was also observed by Plunkett and Lee[30]. Their investigations were limited, however, to applications for metallic materials and the effects of tape boundary conditions were not taken into account.

For the condition where the tape was applied at a distance of 0.5 inches (12.7 mm) from the clamped end (N/L/ = 0.1), Figure 5 shows that the damping effectiveness, although improved, is not as significant as for the above two cases. This is not surprising since, in the first mode of vibration, the most highly stressed region is at the clamped end. With no tape in this region to provide the additional damping mechanism (by shear deformation of the viscoelastic adhesive) the overall improvement is minimal. The experimental results (with scatter) obtained with the impulse hammer technique show fair agreement with finite element analytical predictions. Better agreement is expected if the data on complex shear modulus of the damping layer is available in the form of accurate regression equations. The results shown here are based on estimates from Nomographs.

Loss factor data for the second mode (Figures 4 and 6) beyond T/L = 0.6 for all the three boundary conditions could not be experimentally obtained with the impulse hammer technique because the peaks were almost

flat (damped out) in this region. The high damping ratios predicted by the analytical model for these conditions (beyond T/L = 0.6) also confirm this effect. As such, specimens with a longer cantilever span (instead of the five inches used here) were expected to give more distinguishable resonant peaks for the second mode of vibration. Accordingly, the unidirectional and off-axis graphite/epoxy specimens were tested with an eight inch cantilever span to facilitate complete frequency dependence of the experimental validation of the analytical predictions.

Figures 7 and 8 once again show a comparable improvement in damping for both fixed and free boundary conditions of the damping tape as applied to the unidirectional graphite/epoxy base structure. The damping ratio is not so significant, however, for the off-axis graphite/epoxy specimens (Figures 9 and 10). This is because, with the 20^0 off-axis case the base structure itself exhibited a high intrinsic loss factor (about 0.0134 for mode 1 and 0.0252 for mode 2).

The critical observation that by fixing the constrained layer tape at the clamped end, significantly higher overall damping could be obtained, was further investigated. This has important ramifications by way of added weight trade-offs when such surface damping treatments are planned, for example, in helicopter rotor blade applications. To simulate better the finite element model of the tape being fixed at root, some experiments were repeated by fixing the tape at the root with a clamp along the face of the vise instead of having the tape inside the vise (Figure 1). As shown in Table 2 the damping effectiveness is once again comparably higher than for the free at root boundary condition. (The marginal variations in the loss factor data presented here with the data in Figure 3 is attributed to a different batch of damping tape that was used for these tests). The increased through-the-thickness shear strain in the adhesive as a result of fixing the tape at the root is responsible for the increase in the system damping. This is easily verified by observing the shear strain energy ratio obtained by the 3-D finite element method for the fixed vs free boundary conditions at root, as shown in Figures 11 and 12 for both the first and second modes of vibration.

Similar conclusions on the effects of boundary conditions were reported by Mead and Markus[31], who developed a closed form analytical solution for sandwich beams with fixed, free and simply supported boundary conditions. Their results suggest that the effect of boundary conditions depends on the frequency range, however, and that the maximum system loss factor is not very sensitive to boundary conditions. A direct comparison of the present results with those of Mead and Markus is not possible because the present work is concerned with discontinuous damping layers whose complex shear modulus varies with frequency, whereas Mead and Markus analyzed continuous damping layers whose complex shear modulus is assumed to be constant.

Finally, Figure 13 shows polaroid pictures of the first mode peaks in the frequency response spectrum taken from the screen of the HP3582A spectrum analyzer, for the case where the tape was fixed at the root in conjunction with different lengths of the tape applied to the base structure. The shortening and widening of the peak indicates how the tape is effective in damping resonant vibrations.

CONCLUSIONS

Measurement and predictions show that, for a given composite cantilever beam vibrating in a given mode, there is an optimum damping tape distribution for maximum damping. Significant improvements in damping were predicted and measured when the constraining layer was clamped at the fixed end of the beam. The amount of damping tape (and its added weight) required to produce a given improvement in damping can be significantly reduced by clamping the tape at the fixed end of the beam. The three- dimensional finite element implementation of the modal strain energy method proved to be a powerful analytical tool for predicting damping of such complex systems. Finally, the impulse-frequency response technique is a fast and accurate method for measuring damping in such structures.

ACKNOWLEDGEMENTS

The support of the Army Research Office grant No. DAAL03-88-K-0013 (Program Manager - Dr. Gary Anderson) through a subcontract from the University of Florida is gratefully acknowledged. The authors are also indebted to Dr. Dwayne Nelson of the 3M Company, St. Paul, Minnesota for the time spent in fruitful discussions and for supplying the damping tapes.

REFERENCES

[1] Ross, D., Ungar, E.E., and Kerwin, E.M. Jr., "Damping of Plate Flexural Vibrations by means of Viscoelastic Laminate", Structural Damping, ASME, New York, p. 49-88, 1959.

[2] Jones, D.I.G., "Effect of Free Layer damping on Response of Stiffened Plate Structure", Shock and Vibration Bulletin, Vol. 42, Part II, p. 105, December 1970.

[3] Jones, D.I.G., "Design of Constrained Layer Treatments for Broad Temperature Damping", Shock and Vibration Bulletin, Vol. 44, Part V, p. 1, 1974.

[4] Rogers, L.C., and Nashif, A.D., "Computerized Processing and Empirical representation of Viscoelastic Material Property Data and Preliminary Constrained Layer Damping Treatment Design", Shock and Vibration Bulletin, Vol. 48, Part II, p. 23, 1978.

[5] Jones, D.I.G., Nashif, A.D. and Parin, M.L., "Parametric Study of Multiple-Layer Damping Treatments on Beams", Journal of Sound and Vibration, Vol. 29, No.4, p. 423, 1973.

[6] Nashif, A.D. and Nicholas, T., "Vibration Control by a Multiple-layered Damping Treatment", Shock and Vibration Bulletin, Vol. 41, Part II, p. 121, 1970.

[7] Ely, R.A., and Sangha, K.B., "Prediction and Measurement of Damping of Vibrations of structures by Adhesives", Proceedings of Advancing Technology in Materials and Processes, 30th National SAMPE Symposium and Exhibition, Vol. 30, Anaheim, California, March 19-21, 1985.

[8] Ely, R.A., "Laminated Damped Aircraft Structures", Presented at the ASME Winter Annual Winter Meeting, New Orleans, Louisiana, December 3, 1984.

[9] Sun, C.T., Sankar, B.V. and Rao, V.S., "Damping and Vibration Control of Unidirectional Composite Beams Using Add-On Viscoelastic Materials", 59th Shock and Vibration Symposium, Albuquerque, New Mexico, October 18-20, 1988.

[10] Gibson R.F., Chaturvedi, S.K. and Sun, C.T., "Complex Moduli of Aligned Discontinuous Fiber-Reinforced Polymer Composites", Journal of Materials Science, Vol. 17, p. 3499, 1982.

[11] Gibson, R.F., Sun, C.T. and Chaturvedi, S.K., "Damping and Stiffness of Aligned Discontinuous Fiber Reinforced Polymer Composites", Proceedings of the 23rd AIAA/ASME/ASCE/AHS Structures, Structural Dynamics and Materials Conference, New Orleans, Louisiana, May 10-12, 1982.

[12] Sun, C.T., Chaturvedi, S.K. and Gibson, R.F., "Internal Damping of Short Fiber Polymer Matrix Composites"' presented at the symposium on advances and Trends in Structures and Dynamics (sponsored by NASA Langley Research Center), Washington D.C., October 22-25, 1984, also published in Computers and Structures, Vol. 20, No. 1-3, pp. 391-400, 1985.

[13] Sun, C.T., Gibson, R.F. and Chaturvedi, S.K., "Internal Damping of polymer Matrix Composites Under Off-axis loading", Journal of Materials Science, Vol. 20, p. 2575, 1985.

[14] Suarez, S.A., Gibson, R.F., Sun, C.T. and Chaturvedi, S.K., "The influence of Fiber Length and Fiber Orientation on Damping and Stiffness of Polymer Composite Materials', Experimental Mechanics , 26 (2), pp. 175-184, June 1986.

[15] Sun, C.T., Wu, J.K. and Gibson, R.F., "Prediction of Material Damping in Randomly Oriented Short Fiber Polymer Matrix Composites", Journal of Reinforced Plastics and Composites, Vol. 4, pp. 262-272, July 1985.

[16] Sun, C.T., Wu, J.K. and Gibson, R.F., "Prediction of Material Damping of Laminated Polymer Matrix Composites", proceedings of Vibration Damping Workshop II, Las Vegas, Nevada March 5-7, 1986.

[17] Wu, J.K., "Optimization Of Material Damping and Stiffness of Laminated Fiber-reinforced Composite Structural Elements", Ph.D. Dissertation, Department of Engineering Sciences, University of Florida, Gainsville, Florida, December 1985.

[18] Hwang, S.J. and Gibson, R.F., "Micromechanical Modeling of Damping in Discontinuous Fiber Composites Using a Strain Energy / Finite Element Approach", Journal of Engineering Materials and Technology, 109, pp. 47-52, January 1987.

[19] Hwang, S.J., "Characterization of the Effects of Three Dimensional States of Stress on Damping of Laminated Composites" Ph.D. Dissertation, Mechanical Engineering Department, University of Idaho, May 1988.

[20] Hwang, S.J. and Gibson, R.F., "The Effects of Three Dimensional States of Stress on Damping of Laminated Composites", 34th International SAMPE Symposium, Reno, Nevada, May 8-11, 1989.

[21] Gibson, R.F., Deobald, L.R. and Suarez, S.A., "Laboratory Production Of Discontinuous Aligned Composite Plates Using the Autoclave-style Press Cure", Journal of Composites Technology Research, ASTM, Vol. 7, No. 2, pp. 49-54, 1985.

[22] Suarez, S.A. and Gibson, R.F., "Improved Impulse-Frequency Response Technique for Measurement of Dynamic Mechanical Properties of Composite Materials", Journal of Testing and Evaluation, 15 (2), pp. 114-121, March 1987.

[23] Ungar, E.E. and Kerwin Jr., E.M., "Loss Factors of Viscoelastic Systems in Terms of Strain Energy Concepts", Journal of Acoustical Society of America, 34 (2), pp. 954-958, July 1962.

[24] Johnson, C.D. and Kienholz, D.A., "Finite Element Prediction of Damping in Structures With Constrained Viscoelastic Layers", AIAA Journal, 20 (9), pp. 17-24, September 1982.

[25] Bogner, F.K. and Soni, M.L., "Finite Element Vibration Analysis of Damped Structures", Proceedings of the 22nd Structures, Structural Dynamics and materials Conference, Atlanta, Georgia, Paper No. 81-0489, April 1981.

[26] Bathe, K.J. et al, SAP IV a Structural Analysis Program for Static and Dynamic Response of Linear Systems, College of Engineering, University of California, Berkeley, California, April 1974.

[27] Product Information, "Scotchdamp" Vibration Damping Tapes SJ-2052X Nomograph, Structural Products Department, 3M Center, St. Paul, Minnesota.

[28] Nashif, A.D., Jones, D.I.G. and Henderson, J.P., Vibration Damping, John-Wiley, Interscience, 1985.

[29] Lu, Y.P. and Everstine, G.C., "More on Finite Element Modeling of Damped Composite Systems", Journal of Sound and Vibration, 69 (2), pp. 199-205, 1980.

[30] Plunkett, R. and Lee, C.T., "Length Optimization for Constrained Viscoelastic Layer Damping", Journal of Acoustical Society of America, Vol. 48, pp. 150-161, 1970.

[31] Mead, D.J. and Markus, S., "Loss Factors and Resonant Frequencies of Encastre' Damped Sandwich Beams", Journal of Sound and Vibration, 12 (1), pp. 99-112, 1970.

TABLE 1. Composite structure constituent material properties.

	Density ρ	Longitudinal Modulus E_1	Transverse Modulus E_2	Shear Modulus G_{12}	Poisson's Ratio ν_{12}	Fiber Volume Fraction v_f	Loss Factor (@ 70°F) MODE 1	Loss Factor (@ 70°F) MODE 2
BASE STRUCTURE								
E-Glass Epoxy [16 ply/0°/0.13" thick]	1.90 g/cm^3 (0.07 lb/in^3)	36GPa (5.25MPsi)	11GPa (1.58MPsi)	3GPa (0.44MPsi)	0.28	0.50	0.0040 (@ 140Hz)	0.0035 (@ 880Hz)
Graphite Epoxy [12 ply/0°/0.06" thick]	1.58 g/cm^3 (0.06 lb/in^3)	127.9GPa (18.55MPsi)	10.27GPa (1.49MPsi)	7.31GPa (1.06MPsi)	0.22	0.67	0.0029 (@ 55Hz)	0.0037 (@ 330Hz)
CONSTRAINING LAYER								
Dead Soft Aluminum Foil [Type 1100/0.01" thick]	2.76 g/cm^3 (0.1 lb/in^3)	69GPa (10MPsi)	69GPa (10MPsi)	26GPa (3.79MPsi)	0.32	--	0.033	--
DAMPING LAYER								
3Ms SJ-2052X [ISD-112/0.005" thick]	0.98 g/cm^3 (0.04 lb/in^3)	1.76MPa (255Psi)	1.76MPa (255Psi)	0.59MPa (85Psi)	0.49	--	0.87 (@ 55Hz)	--
	"	3.72MPa (540Psi)	3.72MPa (540Psi)	1.24MPa (180Psi)	"	--	--	0.90 (@ 330Hz)

TABLE 2. Typical experimental data on the influence of tape boundary conditions (at the clamped end of the beam) on system damping for the first and second modes of vibration.

	Loss Factor (Untaped) Glass Epoxy Specimens*	DAMPING WITH DIFFERENT TAPE BOUNDARY CONDITIONS					
		FREE AT ROOT		FIXED (along face of vise)		FIXED (inside vise)	
		Loss Factor (Taped)	Loss Factor Ratio	Loss Factor (Taped)	Loss Factor Ratio	Loss Factor (Taped)	Loss Factor Ratio
MODE 1	0.0040	0.049	12.2	0.070	17.5	0.080	20.3
MODE 2	0.0035	0.029	8.3	0.047	13.3	0.043	12.3

*NOTE: Average of three specimens with N/L = 0.0, T/L = 0.5

DAMPING TAPE – DISTRIBUTION AND BOUNDARY CONDITIONS

T = TAPE LENGTH
L = BEAM LENGTH
N = NO TAPE LENGTH (AT ROOT)

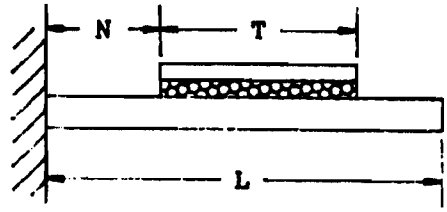

FIXED AT ROOT (TAPE INSIDE VISE)

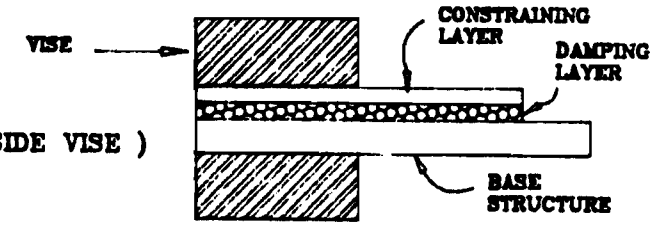

FIXED AT ROOT
(TAPE CLAMPED ALONG FACE OF VISE)

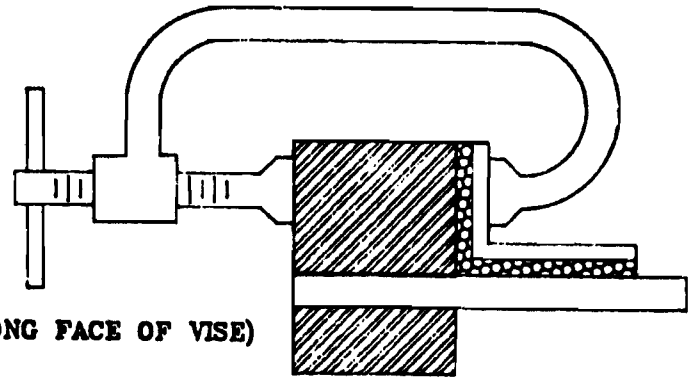

FREE AT ROOT

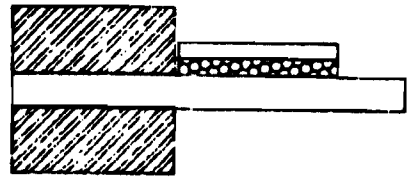

Figure 1. Distribution and boundary conditions of the damping tape applied on one side of the composite base structure.

I.D.	Element	Aspect Ratio (length/thickness)
A	Adhesive Layer	7.144:1
B	Base Structure	0.275:1
C	Constraining Layer	3.572:1

N/L = 0 T/L = 0.6

Number of Elements = 308

Number of Nodes = 904

Number of Degrees of Freedom = 2700

Total Solution Time = 334.79 sec.

(IBM 4341 Main Frame System OS/VS1)

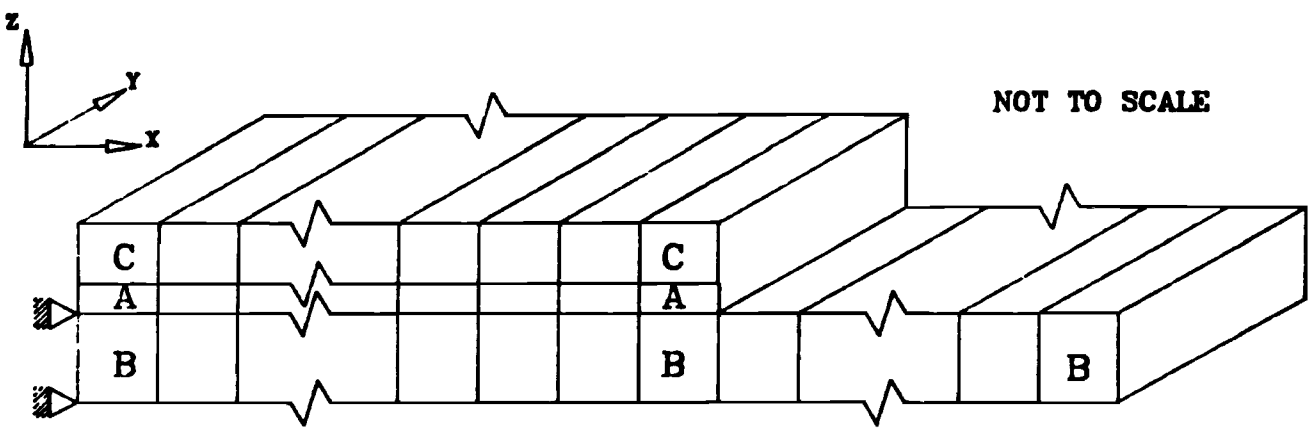

Figure 2. Typical 3-D finite element model of constrained layer damping treatment on a composite base structure (with tape free at clamped end).

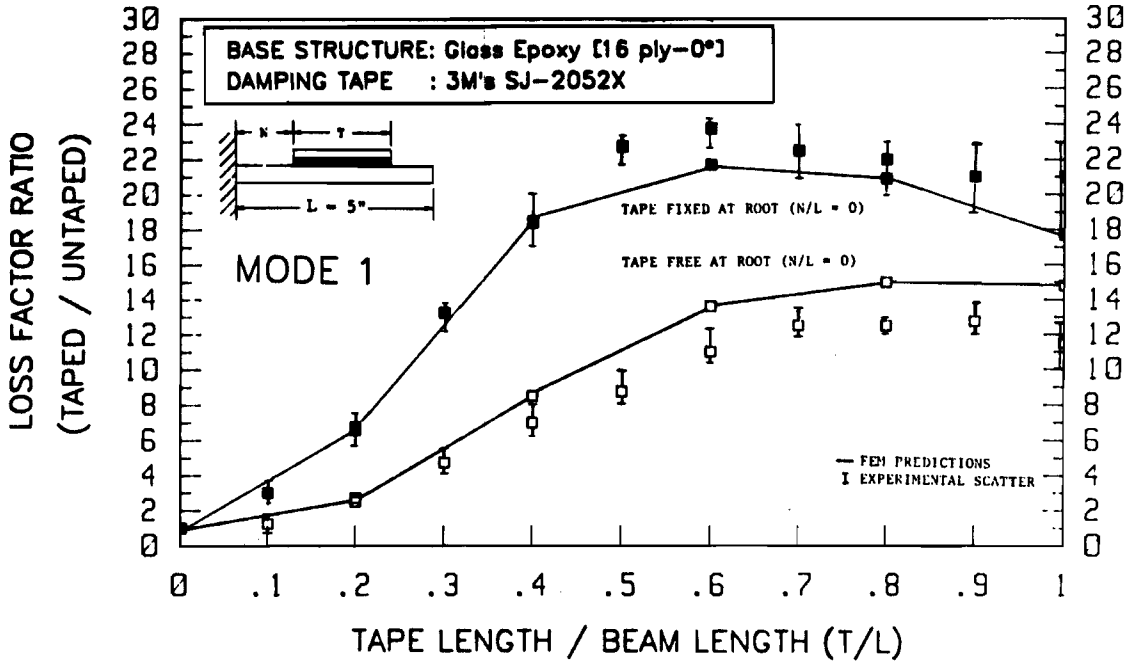

Figure 3. Variation of loss factor with tape length in mode 1 vibration for fixed and free boundary conditions at root, with a unidirectional glass/epoxy composite base structure.

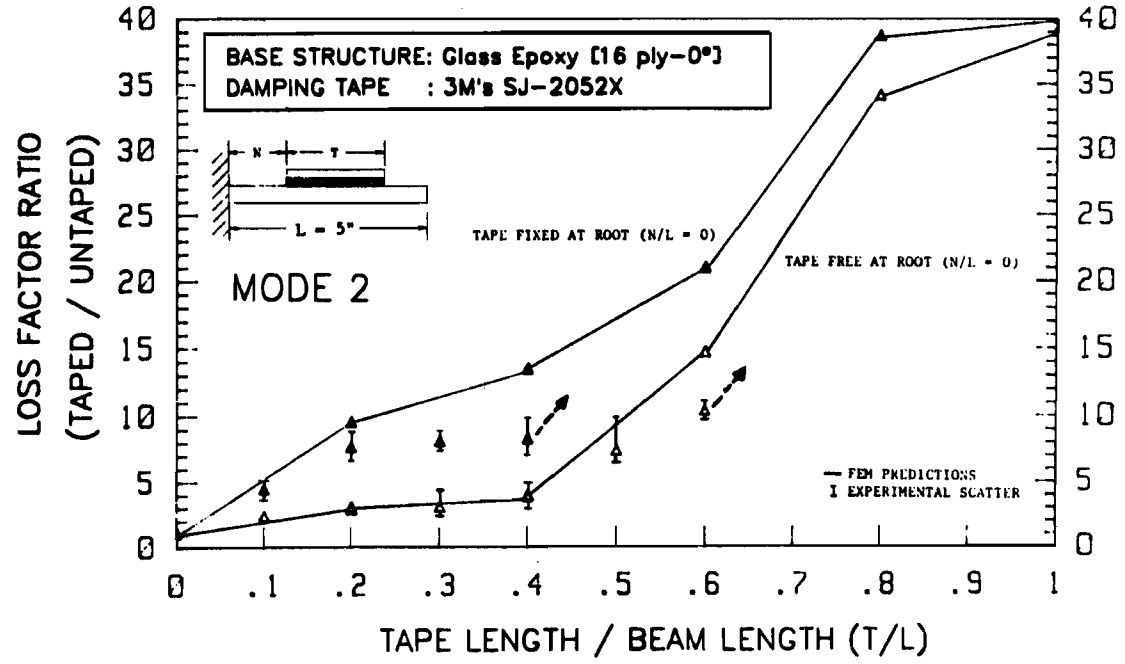

Figure 4. Variation of loss factor with tape length in mode 2 vibration for fixed and free boundary conditions at root, with a unidirectional glass/epoxy composite base structure.

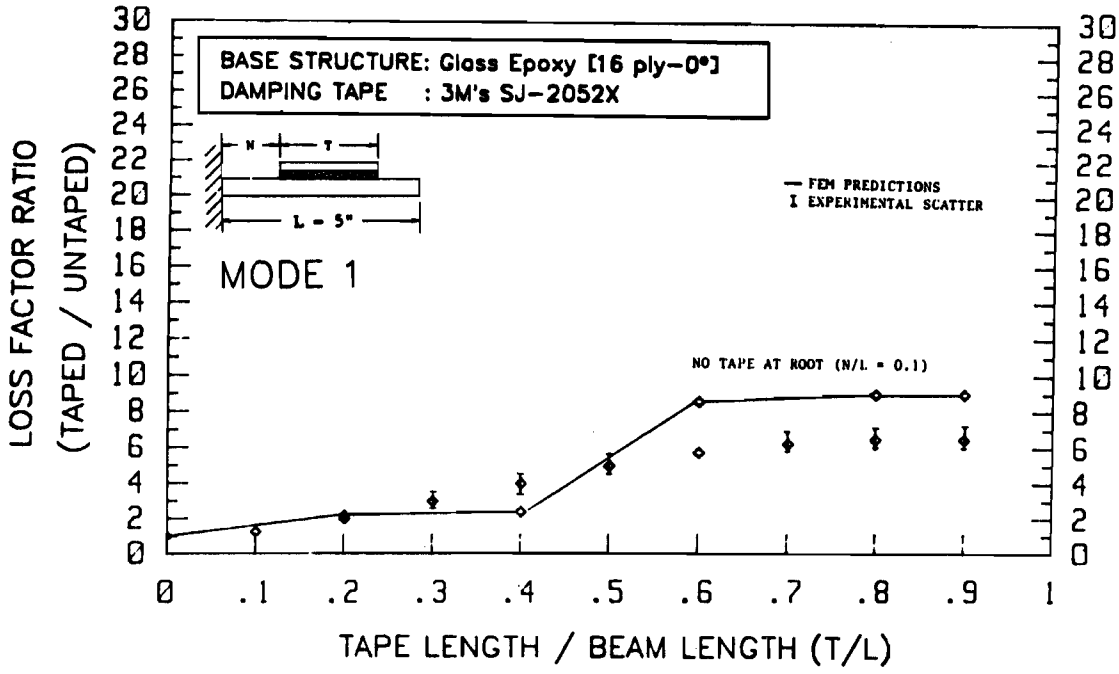

Figure 5. Variation of loss factor with tape length in mode 1 vibration for no tape at root boundary condition, with a unidirectional glass/epoxy composite base structure.

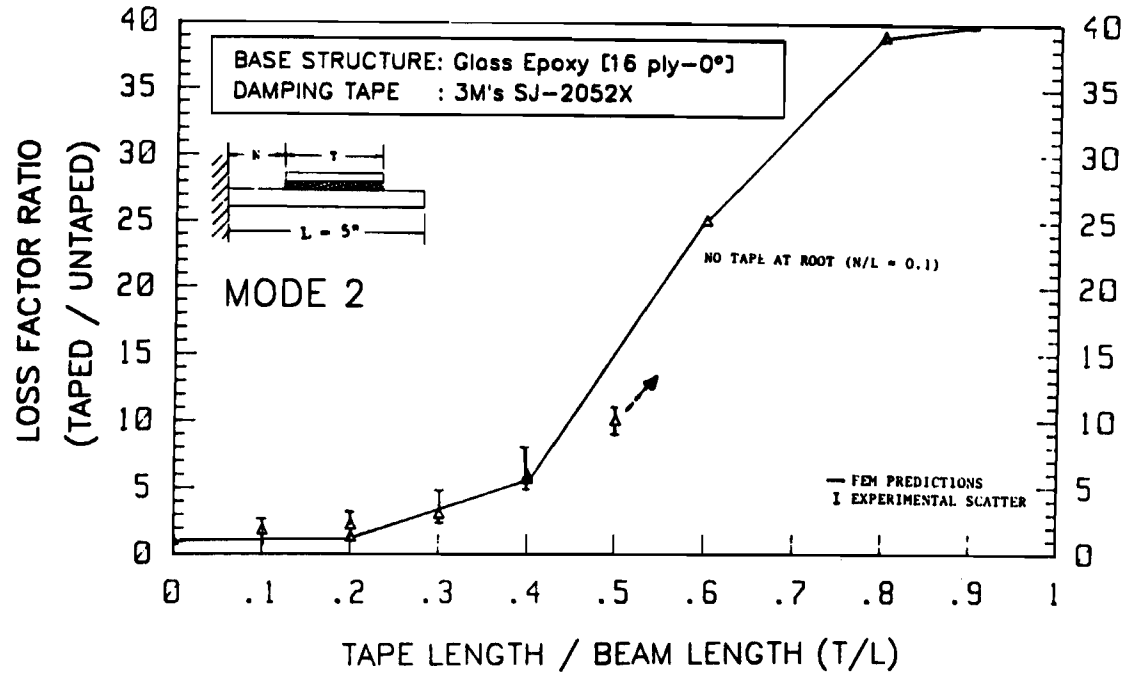

Figure 6. Variation of loss factor with tape length in mode 2 vibration for no tape at root boundary condition, with a unidirectional glass/epoxy composite base structure.

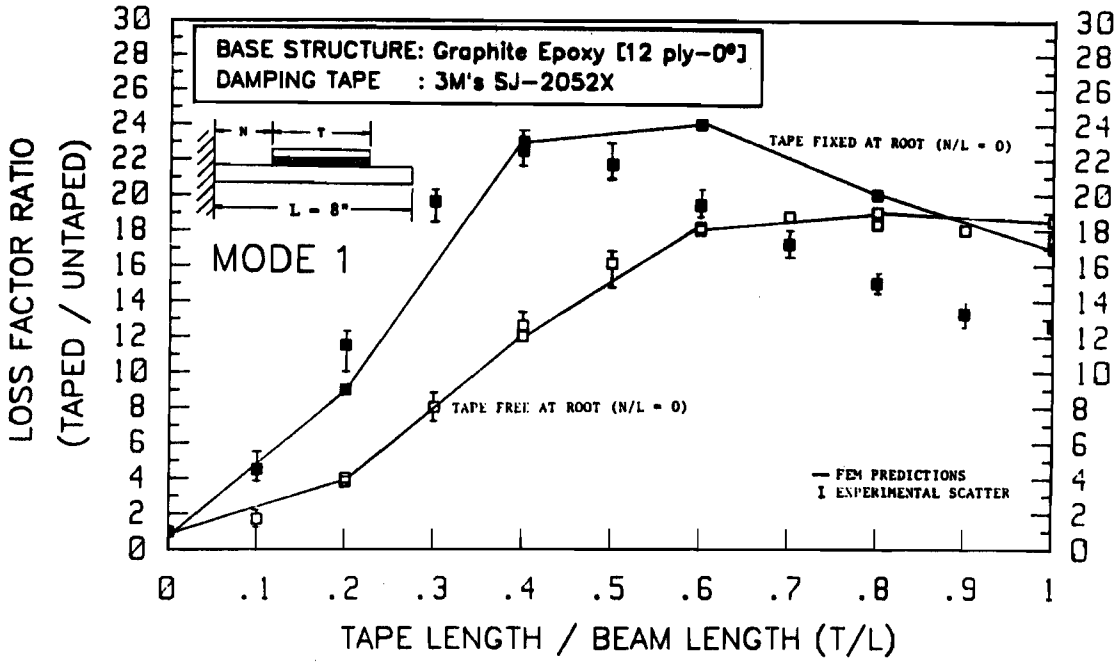

Figure 7. Variation of loss factor with tape length in mode 1 vibration for fixed and free boundary conditions at root, with a unidirectional graphite/epoxy composite base structure.

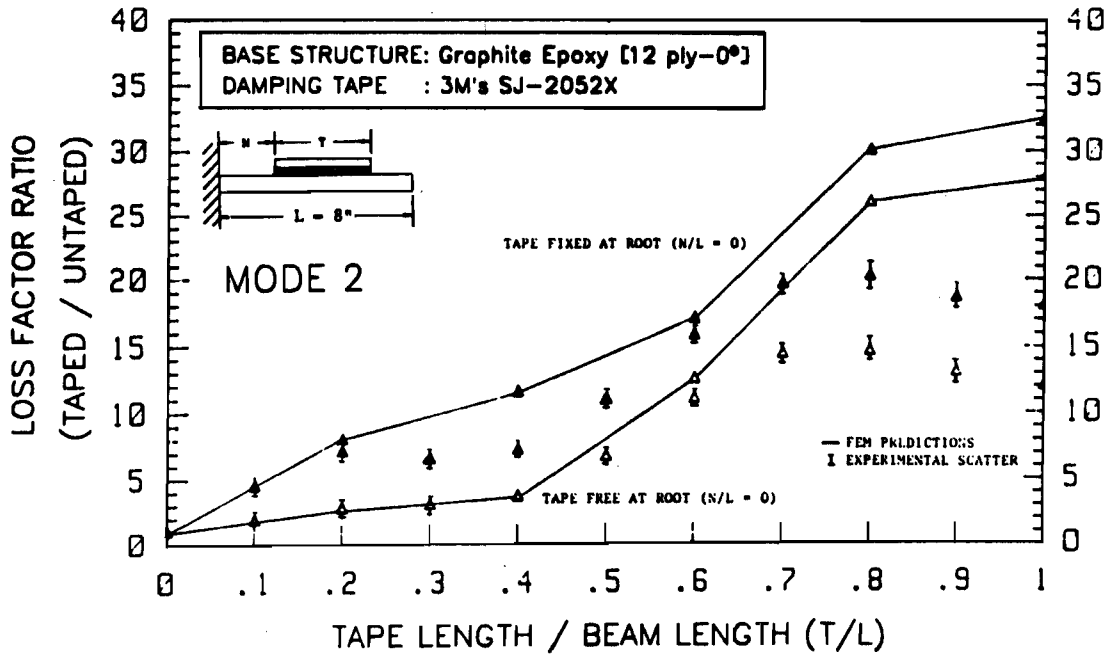

Figure 8. Variation of loss factor with tape length in mode 2 vibration for fixed and free boundary conditions at root, with a unidirectional graphite/epoxy composite base structure.

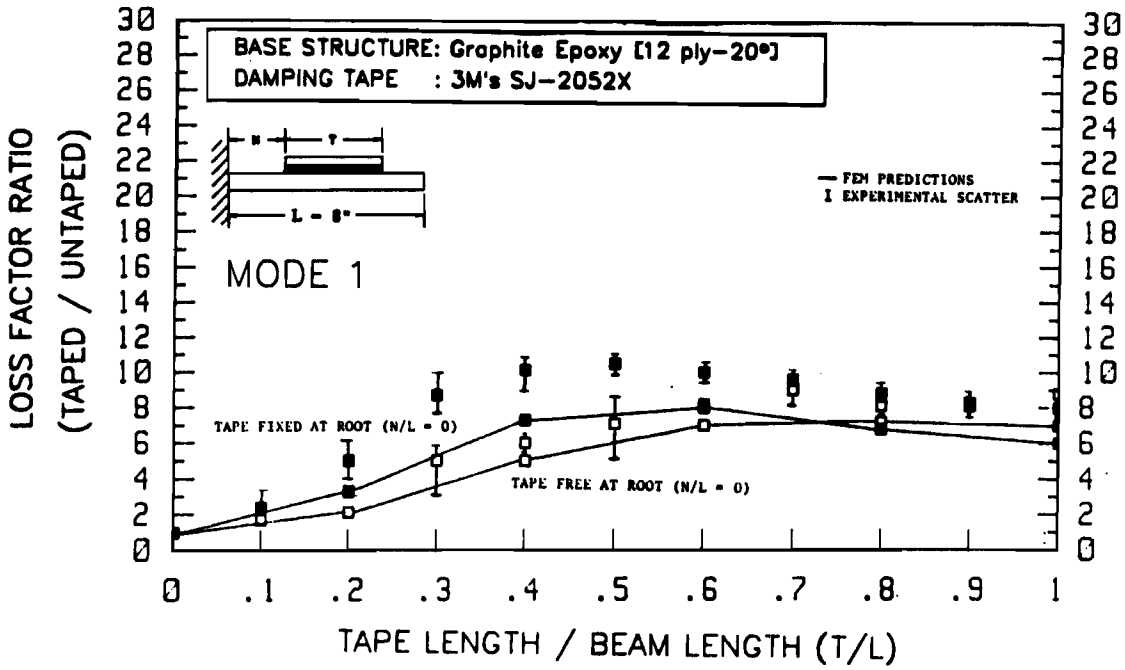

Figure 9. Variation of loss factor with tape length in mode 1 vibration for fixed and free boundary conditions at root, with a 20^0 off-axis graphite/epoxy composite base structure.

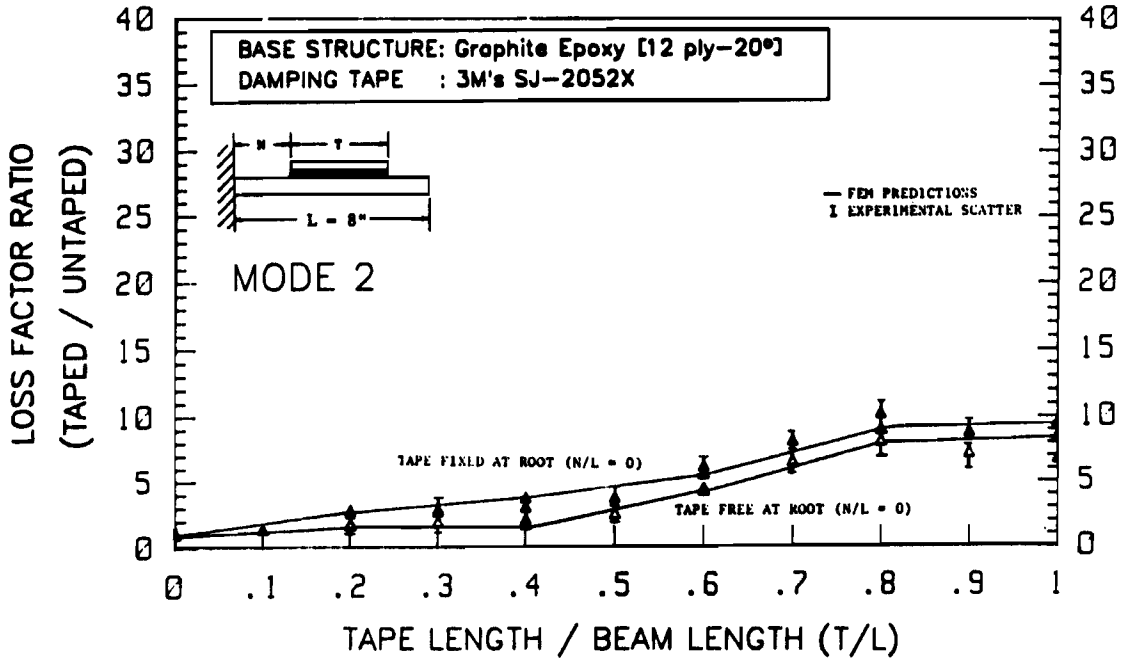

Figure 10. Variation of loss factor with tape length in mode 2 vibration for fixed and free boundary conditions at root, with a 20^0 off-axis graphite/epoxy composite base structure.

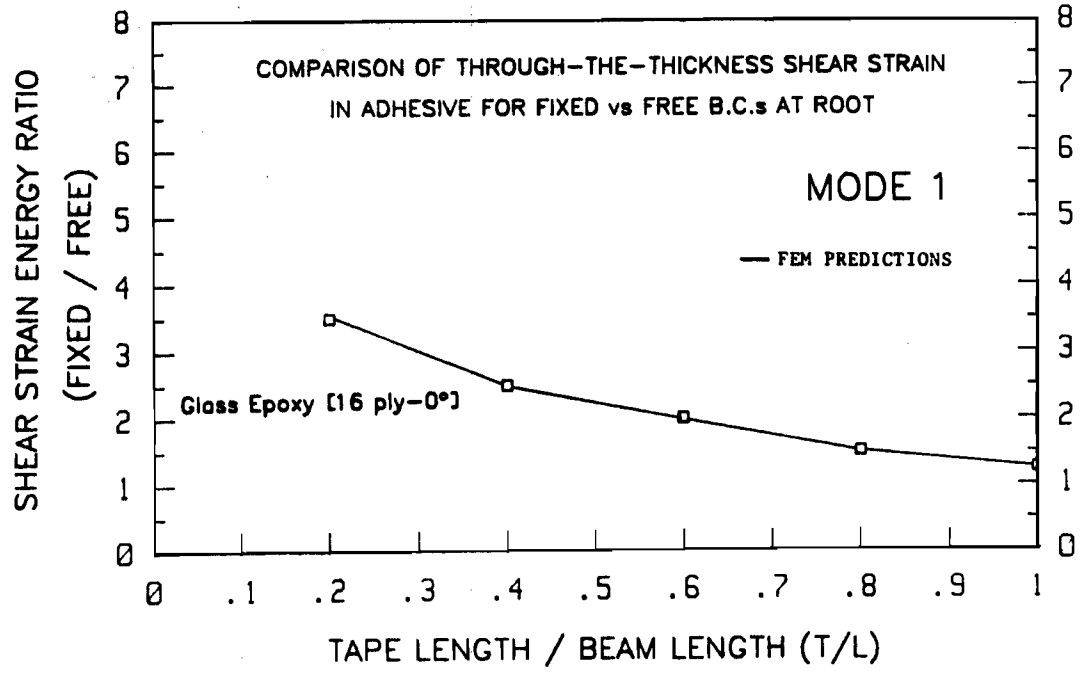

Figure 11. Analytical predictions of through-the-thickness shear strain in adhesive for fixed vs free boundary conditions at root, in mode 1 vibration.

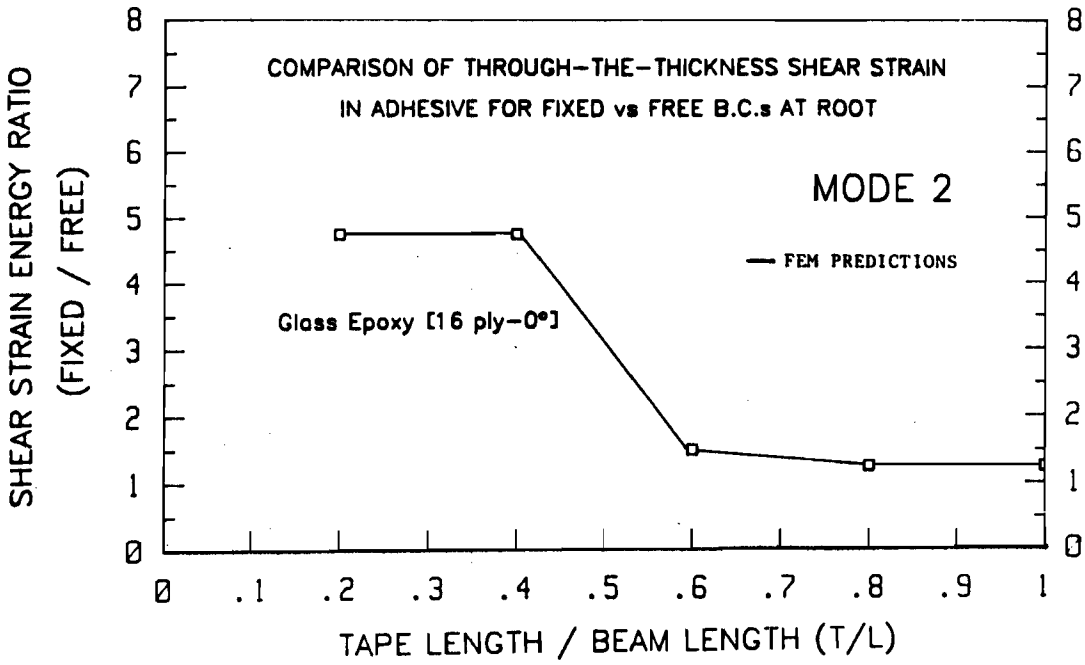

Figure 12. Analytical predictions of through-the-thickness shear strain in adhesive for fixed vs free boundary conditions at root, in mode 2 vibration.

(a) Tape/Beam Length = 0.0
1st Mode Frequency = 135 Hz
Loss factor = 0.004

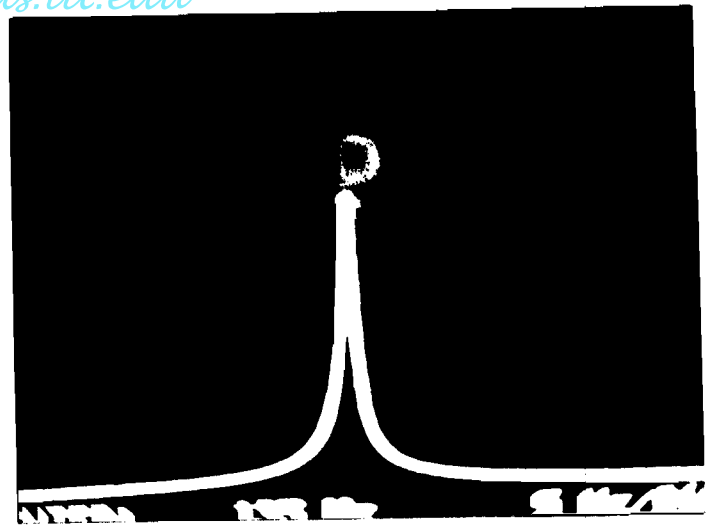

(b) Tape/Beam Length = 0.2
1st Mode Frequency = 137 Hz
Loss Factor = 0.027

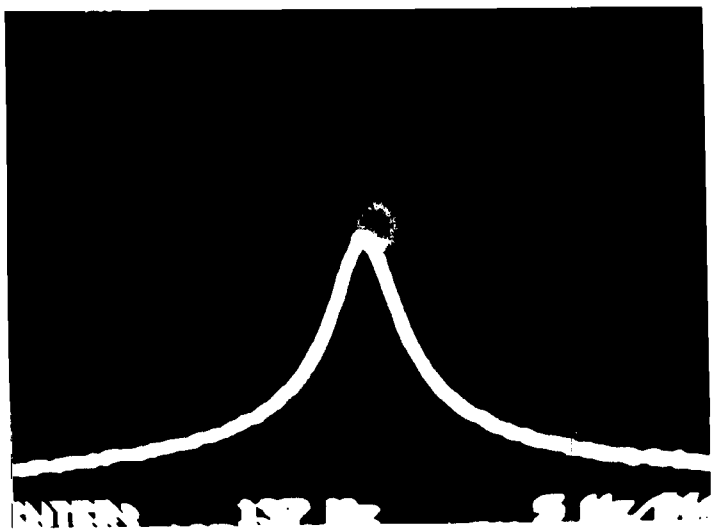

(c) Tape/Beam Length = 1.0
1st Mode Frequency = 147 Hz
Loss Factor = 0.083

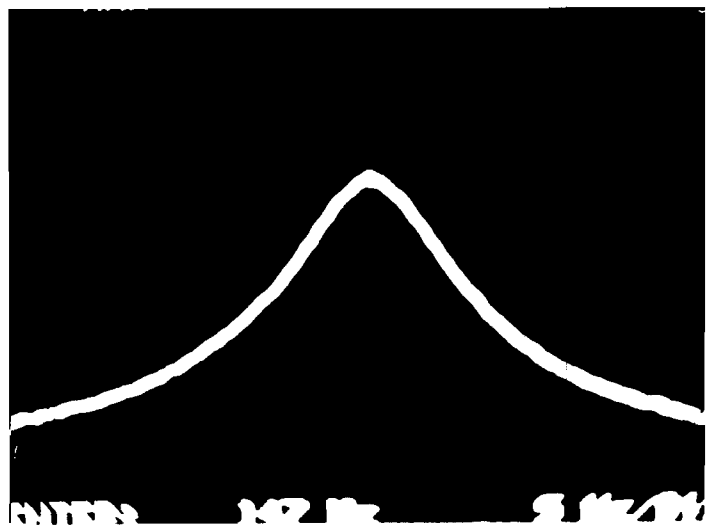

Figure 13 (a,b,and c). Shortening and widening of the 1st mode peak (as observed on the screen of the spectrum analyzer) for different tape/beam length ratios indicating how the tape is effective in damping resonant vibrations of the glass/epoxy composite specimens.